Appl Microbiol Biotechnol (2013) 97:8291–8306
DOI 10.1007/s00253-013-5092-6

Growth, lipid production and metabolic adjustments in the euryhaline eustigmatophyte *Nannochloropsis oceanica* CCALA 804 in response to osmotic downshift

Dipasmita Pal · Inna Khozin-Goldberg · Shoshana Didi-Cohen · Alexei Solovchenko · Albert Batushansky · Yuval Kaye · Noga Sikron · Talya Samani · Aaron Fait · Sammy Boussiba

Received: 1 April 2013 / Revised: 27 June 2013 / Accepted: 1 July 2013 / Published online: 25 July 2013

Abstract We investigated the effects of osmotic downshift induced by the transfer of *Nannochloropsis oceanica* CCALA 804 from artificial seawater medium (27 g L^{-1} NaCl) to the same medium without NaCl or freshwater modified BG-11 medium (mBG-11) as a function of photosynthetically active radiation (170, 350, or 700 μmol photon m^{-2} s^{-1}). Alterations in growth, total fatty acid (FA) content and FA composition of individual lipid classes, and in relative contents of metabolites relevant to osmotic adjustments were studied. Cells displayed remarkable tolerance to the osmotic downshift apart from some swelling, with no substantial lag or decline in cell division rate. Biomass accumulation and chlorophyll a content were enhanced upon downshifting, especially under the highest irradiance. The highest chlorophyll a and eicosapentaenoic acid (EPA) biomass and culture contents were determined in the cultures grown in mBG-11. Two days after transfer to 0 g L^{-1} NaCl, the proportion in total acyl lipids of the major chloroplast galactolipid monogalactosyldiacylglycerol, a major depot of EPA, increased twofold, along with a modest change in the proportion of digalactosyldiacylglycerol (DGDG). EPA percentage decreased in DGDG and increased in the extraplastidial lipid phosphatidylethanolamine. Metabolite profiling by GC–MS analysis revealed a sharp decrease in metabolites potentially involved in osmoregulation, such as mannitol and proline, while proline-cycle intermediates and some free sugars increased. The stress-induced polyamine spermidine decreased *ca*. one order of magnitude, while its catabolic product—the non-protein amino acid γ-amino butyric acid—increased twofold, as did the stress-related sugars trehalose and talose. Biochemical mechanisms governing osmotic plasticity and implications for optimization of EPA production by *N. oceanica* CCALA 804 under variable cultivation conditions are discussed.

Keywords EPA · Euryhaline microalga · MGDG · *Nannochloropsis* · Osmolyte · Salinity · TFA

Introduction

Planktonic heterokont microalgae of the genus *Nannochloropsis* belong to the relatively recently described algal class Eustigmatophyceae (Hibberd 1981), so far represented by several members (Andersen et al. 1998; Krienitz et al. 2000; Fawley and Fawley 2007; Suda et al. 2002; Vieler et al. 2012; Jinkerson et al. 2013). Most of them are marine species; in addition, the freshwater *Nannochloropsis limnetica* has been isolated from inland freshwater bodies (Krienitz et al. 2000; Fietz et al. 2005; Fawley and Fawley 2007), indicating a diversity of natural habitats for *Nannochloropsis* microalgae with respect to salinity level.

Both marine and freshwater *Nannochloropsis* species produce the n-3 (omega-3) long-chain polyunsaturated fatty acid (LC-PUFA) eicosapentaenoic acid (EPA, 20:5 n-3) as a major LC-PUFA of the chloroplast membrane galactolipids

Electronic supplementary material The online version of this article (doi:10.1007/s00253-013-5092-6) contains supplementary material, which is available to authorized users.

D. Pal · I. Khozin-Goldberg (✉) · S. Didi-Cohen · A. Batushansky · Y. Kaye · N. Sikron · T. Samani · A. Fait · S. Boussiba
French Associates Institute of Agriculture and Biotechnology of Drylands, J. Blaustein Institutes for Desert Research, Ben-Gurion University of the Negev, Midreshet Ben-Gurion 84990, Israel
e-mail: khozin@bgu.ac.il

A. Solovchenko
Department of Bioengineering, Faculty of Biology, Moscow State University, GSP-1, Moscow 119234, Russia

A. Solovchenko
Timiryazev Institute of Plant Physiology, Russian Academy of Sciences, Botanicheskaya ul. 35, Moscow 127276, Russia

(Sukenik 1999; Fietz et al. 2005). Due to their high EPA content, various species of *Nannochloropsis* are widely used in aquaculture (Renaud et al. 1991; Sukenik et al. 1993b; Renaud and Parry 1994) and hold promise as an efficient source of EPA for human nutrition. Accumulating experimental evidence indicates that these robust microalgae can cope with severe variations in growth conditions, such as salinity level, nutrient deficiency, light intensity, and being cultivated in various types of cultivation facilities, both indoor and outdoor (Boussiba et al. 1987; Renaud et al. 1991; Renaud and Parry 1994; Fisher et al. 1998; Zou et al. 2000; Rodolfi et al. 2009; Sukenik et al. 2009; Pal et al. 2011; Simionato et al. 2011). Species of the genus *Nannochloropsis* can acclimate to a wide range of irradiances with no adverse effects on growth (Pal et al. 2011; Simionato et al. 2011). In addition, the ability to overproduce storage lipid triacylglycerols (TAG) under nitrogen starvation and tolerance to high irradiances make *Nannochloropsis* species a promising feedstock for biofuel production (Rodolfi et al. 2009) and a leading phototrophic microorganism for the production of biofuels on an industrial scale (Jinkerson et al. 2013). We have previously shown that lower salinity levels (13 g L^{-1}) tend to improve major growth parameters and EPA content in nitrogen-replete cultures of a *Nannochloropsis* sp., and enhance total fatty acid (TFA) production in nitrogen-depleted cultures (Pal et al. 2011). However, the mechanisms governing the positive response to osmotic downshift have never been studied.

Marine species of the genus *Nannochloropsis*, such as *Nannochloropsis oculata*, *Nannochloropsis salina*, *Nannochloropsis gaditana*, etc. (Hibberd 1981; Suda et al. 2002), inhabit coastal waters and estuaries where planktonic microalgae frequently encounter widely varying mixtures of fresh and salt water during the tidal cycle. The microalgae from such environments possess rapidly responding mechanisms that allow their cell walls to swell without rupturing under hypotonic conditions and prevent water loss at increased salinities (Ahmad and Hellebust 1984, 1986; Kirst 1989). The need to cope with fluctuations in external salinity and intracellular osmotic conditions led to the acquisition of metabolic plasticity by microalgae inhabiting estuaries, allowing for rapid acclimation to variable osmolarity (Bisson and Kirst 1995). The acclimation mechanisms governing metabolic adjustments might include the production of versatile osmoregulatory compounds, such as proline and glycine betaine (Brown and Hellebust 1980; Ahmad and Hellebust 1984; Liu et al. 2000), and various polyols, such as sorbitol, ribitol (Garza–Sánchez et al. 2009; Gustavs et al. 2010), and mannitol (Brown and Hellebust 1980; Dittami et al. 2012).

Modifications in lipid metabolism, including changes in membrane lipid unsaturation level, are thought to play a significant role in the salt tolerance of photosynthetic organisms, including microalgae (Harwood 1998). Marine planktonic microalgae might employ various strategies with respect to membrane unsaturation, perhaps depending on water depth, salinity, or cell wall strength, as well as other environmentally hostile conditions. The decreased level of fatty acid (FA) unsaturation at higher salinity is assumed to be associated with a decrease in membrane permeability and fluidity to prevent leakage of compatible solutes out of the cell and diffusion of potentially harmful ions into the cell (Chen et al. 2008; Lu et al. 2012).

Apart from being of ecological importance, from a biotechnological standpoint, tolerance or promiscuity of microalgae to sudden osmotic downshift is an important feature for cultivation in open shallow ponds where rainfall can unpredictably create extreme hypoosmotic conditions. Moreover, a previous study on nitrogen-replete cultures of a *Nannochloropsis* sp. (Pal et al. 2011) showed that brackish salinities (13.5 g L^{-1} NaCl) promote growth and enhance EPA production as compared to 27 and 40 g L^{-1} NaCl. In the present work, we characterized the strain in that previous work as *Nannochloropsis oceanica* strain CCALA 804 by molecular means and focused on the effects of osmotic downshift to 0 g L^{-1} NaCl in artificial seawater (ASW), as well as transfer to freshwater modified BG-11 medium (mBG-11) on growth, TFA content, and EPA production in nitrogen-replete cultures under different levels of photosynthetically active radiation (PAR). To elucidate the biochemical mechanisms governing tolerance to low osmotic conditions, we examined the changes in distribution of acyl lipid classes and metabolites relevant for osmoregulation.

Materials and methods

Strain

The investigated strain was *Nannochloropsis* sp. strain CCALA 804 [ZMORA/1995, Culture Collection of Autotrophic Organisms (CCALA), Institute of Botany, Academy of Sciences of the Czech Republic]. Molecular phylogenetic characterization of the strain was carried out.

Molecular characterization

DNA was extracted using the CTAB procedure (Doyle and Doyle 1987). The ribulose-1,5-bisphosphate carboxylase/oxygenase large subunit (rbcL) sequence of *Nannochloropsis* sp. CCALA 804 was amplified by PCR using PrimeSTAR® HS (Premix; Cat. no. R040A, Takara Bio Inc., Otsu, Shiga, Japan) according to the manufacturer's protocol.

The following forward and reverse primers that were designed according to conserved regions of available *Nannochloropsis* rbcL sequences available in the National

Center for Biotechnology Information (NCBI) were used for PCR and sequencing:

rbcL F : TCTGGTGAAGTTAAAGGTTCTTACCT
rbcL R : CTGTTGATGTATAGTTGAAAGCAATATC

PCR amplified a 721-bp DNA fragment using these primers; the PCR product was purified from a 1 % agarose electrophoresis gel by the Zymoclean Gel DNA Recovery Kit (Zymo Research, Irvine, CA). Direct sequencing of the PCR products was performed using the 3500xL Genetic Analyzer (Applied Biosystems, Hitachi, Japan). The obtained sequence was aligned with the rbcL DNA sequences of *Nannochloropsis* species deposited in NCBI, and a phylogram was constructed with the Kyoto University ClustalW multiple sequence alignment program (http://www.genome.jp/tools/ clustalw/), using unweighted pair group method with arithmetic mean (UPGMA) with branch length.

Culture conditions

The strain was cultivated in an ASW-based medium (Pal et al. 2011) supplemented with either 0 or 27 g L^{-1} NaCl, or in mBG-11 (Recht et al. 2012). ASW without NaCl was designated sodium chloride-free medium (SFM). Electrical conductivity (EC) was measured with a CyberScan CON 11/110 conductivity meter (Eutech Instruments, Thermo Scientific, Singapore) and amounted to 2.5, 11.7, and 49.8 mS, corresponding to 1.3, 5.8, and 24.9 g L^{-1} total dissolved solids (TDS) in mBG-11, SFM and ASW, respectively. The initial nitrate content was 1.5 g L^{-1} in all of the media; KNO_3 was supplied as a nitrate source in ASW and SFM, and $NaNO_3$ in mBG-11. The nitrate content in the medium, as estimated by colorimetric nitrate kit with test strips (Cat. no. 1.10020.0001; Merck, Darmstadt, Germany; range of detection 10–500 mg L^{-1} NO_3), was depleted within 4 to 5 days in batch cultivation, prior to the stationary phase.

Cultures were grown in 1-L glass columns (6 cm internal diameter) placed in a temperature-controlled water bath at 25 °C and bubbled with a mixture of 2 % (*v*/*v*) CO_2 in air under continuous irradiance with the following photon flux densities: 170 μmol m^{-2} s^{-1} (low light, LL), 350 μmol m^{-2} s^{-1} (medium light, ML), and 700 μmol m^{-2} s^{-1} (high light, HL). The initial semi-continuous cultures were diluted daily with fresh ASW [to 15 mg L^{-1} chlorophyll (Chl) *a*; biomass content 0.8 g L^{-1} ; *ca.* 0.2×10^9 cell mL^{-1} grown under170 μmol m^{-2} s^{-1}] (Pal et al. 2011). At the start of each experiment, cells grown in ASW were harvested by centrifugation (1,200×*g* for 5 min), washed twice in double-distilled water (DDW), and resuspended in the corresponding medium to the initial Chl *a* concentration and biomass content of 15 mg L^{-1} and 0.8 g L^{-1}, respectively. Under the specified conditions, at least three independent experiments were carried out for each treatment with repeats in duplicate columns. Growth was estimated based on the following parameters: volumetric content of Chl *a*, cell number, and dry weight (DW) (Pal et al. 2011). For DW determination, a 5-mL aliquot of the cell suspension was diluted in five volumes of DDW, and filtered through pre-weighed 47-mm glass fiber paper filters (Cat. no. 13400–47————Q; Glass Fibre Prefilter, Sartorius Stedim Biotech GmbH, Gottingen, Germany). The filters were then dried to a constant weight (8 min in a household microwave oven at 30 % maximal power).

Lipid extraction and analyses

Lyophilized biomass samples (50 mg) were vortexed with 0.2 mL dimethyl sulfoxide (DMSO) in the presence of 10 to 15 glass beads (2 mm diameter) for 10 min at 80 °C. Lipids were further extracted and separated into individual classes by thin-layer chromatography according to Khozin-Goldberg et al. (2002). The FA profile and contents of individual lipid classes were determined as FA methyl esters (FAME) by GC–FID.

GC analysis of FA composition and content

Direct transmethylation was performed by incubating freeze-dried biomass or lipid extracts in dry methanol containing 2 % (*v*/*v*) H_2SO_4 at 80 °C for 1.5 h under argon atmosphere with continuous stirring. Heptadecanoic acid (C17:0; Cat. no. 51610; Fluka, Buchs, Switzerland) was added as an internal standard. FAME were quantified on a Trace GC Ultra (Thermo, Milan, Italy) equipped with a flame ionization detector and a programmed temperature vaporizing (PTV) injector as previously described (Pal et al. 2011).

Metabolite analysis by GC–mass spectrometry

A 10-mg (DW) sample of biomass which had been frozen in liquid nitrogen and stored at −80 °C was extracted for metabolite analysis according to Lisec et al. (2006) with slight modifications. The sample was homogenized in a mixer mill (MM 400, Retsch, Haan, Germany) in the presence of three metal beads (2.5 mm) in five consecutive 1-min grinding cycles using tools that were pre-cooled in liquid nitrogen. Homogenized samples were extracted with 500 μL methanol by vortexing, and then 750 μL chloroform was added. Finally, 1.500 μL double-distilled water was added to achieve phase separation and partition the polar metabolites to the upper methanol/water phase; 400 μL of this upper phase was dried in a vacuum concentrator (Eppendorf Concentrator Plus, Hamburg, Germany), followed by derivatization and injection for GC–mass spectrometry (MS) analysis (Lisec et al. 2006).

Metabolite analysis by GC–MS was performed essentially as described in Roessner et al. (2001) with slight modifications (Bai et al. 2012) on a GC 8000 gas chromatograph equipped with the PTV injector and a mass spectrometer (Trace GC Ultra, Thermo Electron Corp., Rodano (MI), Italy). Derivatized metabolites were resolved on a VF-5ms column (30 m, 0.25 mm, 0.25 μm; Agilent, Santa Clara, CA) using a splitless mode of injection (Bai et al. 2012). A split method of injection (1:32) was employed when specified. Chromatograms were analyzed, and data were processed using Xcalibur 2.0.7 software. The GC–MS library (GMD, http://gmd.mpimp-golm.mpg.de/) was used for peak identification. The median of the sample's total fragments, obtained via TagFinder04 software 1.0, was used for normalization (Luedemann et al. 2008).

Statistical analysis

ANOVA and Student's *t* test for significance with a confidence interval of 95 % were applied using the freely distributed statistical software Multi-Experimental Viewer (MeV 4.8.0). The relative content of metabolites was visualized by heat-map using ggplot2 package for freely distributed R software (version 2.15.1) (http://www.springer.com/statistics/computational+statistics/book/978-0-387-98140-6).

Results

Molecular phylogenetic characterization of the strain

Species in the genus *Nannochloropsis* cannot be morphologically differentiated by either light or electron microscopy, and therefore, molecular techniques such as DNA sequence analysis are implemented to discriminate between species (Andersen et al. 1998; Suda et al. 2002). Although the 18S rDNA gene has been used for species characterization in the genus *Nannochloropsis* (Andersen et al. 1998), we could not find enough sequence variability to distinguish between the different species (data not shown). The rbcL gene has been suggested as a more reliable candidate for molecular characterization of the *Nannochloropsis* species with over three times more variability than in the 18S rDNA (Suda et al. 2002; Fawley and Fawley 2007). We generated the rbcL genomic sequence from the *Nannochloropsis* sp. CCALA 804 (ZMORA/1995; GenBank accession No KF152949) and aligned it to those of *Nannochloropsis* species *N. gaditana*, *Nannochloropsis granulata*, *N. limnetica*, *Nannochloropsis maritima*, *N. oceanica*, *N. oculata*, and *N. salina* acquired from NCBI (see Fig. S1). Analysis of the generated rbcL sequence included 667 characters, with 97 variable sites. All variable sites were found to be identical to those in *N. oceanica*.

The alignment data were used for phylogenetic analyses and to construct a phylogram, using the UPGMA method (Fig. S1). In the constructed phylogram, the *Nannochloropsis* species *N. oceanica* and *N. maritima* were clustered together The published rbcL sequences of *N. oceanica* and the rbcL sequence of the *Nannochloropsis* species used in this study were found to be identical. Therefore, we concluded that the *Nannochloropsis* sp. CCALA 804 used in this study can be taxonomically assigned to *N. oceanica*.

Comparison of *N. oceanica* CCALA 804 growth patterns and TFA production in nutrient media with different osmolarities

To evaluate the effects of osmotic downshift on major growth parameters and EPA production under different PAR levels, and to explore the feasibility of culturing *N. oceanica* CCALA 804 in freshwater media, we attempted to grow the alga in ASW without NaCl (SFM) as well as in mBG-11, often used for cultivation of freshwater Eustigmatophytes, such as *Monodus subterraneus* (Khozin-Goldberg et al. 2002). Exposure of *N. oceanica* CCALA 804 grown in ASW to the hypotonic conditions of mBG-11 and SFM (for EC and TDS values, see "Materials and methods") resulted in cell enlargement and a change in shape, generally from oval to round, likely because of increased osmotic water inflow (Fig. 1); cells, however, did not burst in either mBG-11 or SFM. Cells at the mid-logarithmic stage in mBG-11 and SFM averaged 8–10 μm in diameter; 4- to 8-μm oval cells were abundant in the ASW. Transferring the cells from ASW to either mBG-11 or SFM did not result in any substantial lag in growth, as demonstrated by measuring three major growth parameters: biomass (DW, mg mL-1), Chl *a* content in the culture, and cell concentration, indicating high adaptability of *N. oceanica* CCALA 804 to osmotic downshift. Chl *a* content in the cultures grown in SFM did not differ substantially from that in ASW, except for the stationary-phase cultures under HL, where Chl *a* content was higher in SFM than in ASW (Fig. 2). Moreover, the decrease in Chl *a* content that occurred under HL vs. LL and ML was less evident in the SFM vs. ASW culture. However, the highest Chl *a* content (*ca*. 240 mg L^{-1}) was found in the mid-stationary phase cultures in mBG-11 under LL and ML (Fig. 2). Under HL, the culture in mBG-11demonstrated the sharpest increase in Chl *a* in the log phase, but its content leveled off earlier than in cultures grown in the same medium under lower PAR. Notably, the final volumetric contents of Chl *a* achieved by the cultures grown in ASW under all light regimes were about 30 to 40 % higher than those obtained in our previous research (Pal et al. 2011), when ASW medium was supplied with 30 % less (1.0 g L^{-1}) potassium nitrate. Thus, amendment of the nitrate concentration positively affected final Chl *a* content in

culture, in correlation with the amount of nitrogen source provided.

As demonstrated in Solovchenko et al. (2011), the same strain responds to environmental stress by increasing the total carotenoid (Car)/Chl *a* ratio. In ASW, a dramatic increase in Car/Chl ratio was apparent in the absorption spectra of the total pigment extracts of *N. oceanica* recorded during the experimental period. Indeed, an increase in amplitude in the blue part of the red maximum absorption spectra of the pigments, normalized to Chl *a*, was demonstrated (Fig. 3, curves 3 and 3–1). In contrast, after 7 days of cultivation under the same irradiance, the magnitude of this increase was much lower in the pigment extracts of the cells transferred to SFM (Fig. 3, curves 2 and 2–1), suggesting that the cells grown in SFM are exposed to more favorable conditions than those cultivated in ASW.

There was no significant difference in specific growth rate (μ) calculated on a cell-concentration basis (Fig. 2): μ=0.7–0.77 day^{-1} in SFM or ASW under LL and ML. Under HL, the cultures in mBG-11 exhibited the highest μ of 1.15 day^{-1} (despite a 1-day lag) as compared to 1.0 and 0.97 day^{-1} in SFM and ASW, respectively. A noticeable difference was found between the cultures grown in SFM and ASW under HL: by day 2 after the shift, more cell divisions occurred in ASW, whereas the final cell concentration was higher in SFM (Fig. 2), presumably because of the transient acclimation period required for metabolic adjustments under conditions of HL combined with osmotic downshift.

The biomass-accumulation pattern in all media followed a similar increasing trend during the time course of the experiment. Increasing PAR (HL) resulted in higher biomass contents in the stationary phase regardless of the medium (Fig. 2). The cultures in SFM reached the highest biomass concentration (5.4–8.9 mg mL^{-1} DW) as compared to ASW and mBG-11 (4.7–7.1 and 5.0–7.0 mg mL^{-1}, respectively) under all light regimes. Under ML, biomass production was lower in mBG-11 than in ASW or SFM, whereas under LL and HL, it was similar to ASW (Fig. 2). The highest average biomass productivity was recorded in SFM, regardless of irradiance (Fig. 4). We did not detect any substantial changes in the pattern or quantitative parameters of biomass accumulation in ASW as compared to our previous research performed with 30 % lower initial nitrate content (Pal et al. 2011). Since neither biomass culture contents nor final cell number were altered, our findings may imply that the added supply of nitrate enhanced mainly chloroplast pigment content (on both a biomass and cellular basis). As shown below, a lack of NaCl supported more efficient biomass production but with decreased TFA content, whereas the cultures in ASW had accumulated significant amounts of TFA by the end of the experiment (Table 3, Fig. 2).

TFA accumulation patterns in the cultures under different PAR levels (Fig. 2) followed the same trend as biomass production, with HL enhancing TFA production. However, the highest biomass accumulation in SFM under HL was associated with reduced TFA content in the culture relative to that in ASW. Similarly, cultivation in mBG-11 resulted in decreased TFA production as compared to ASW and SFM. Due to the higher culture content of TFA and lower final cell number in ASW under HL (Fig. 2), the cells grown continuously in ASW possessed almost twice the TFA content (1.30 pg cell^{-1}) of those grown in SFM (0.76 pg cell^{-1}) at the end of the experiment (Fig. S2). Under HL, 2 days after the osmotic downshift, the cells in mBG-11 had *ca*. twofold higher Chl *a* content (0.092 pg cell^{-1}) than those in ASW and SFM, and it remained at that level until the end of the experiment. In contrast, at the cellular level, DW and TFA content (Fig. S2) increased during growth in ASW vs. SFM.

Average TFA productivity (expressed as the average increase in TFA culture content over the period studied) increased at higher PAR regardless of the medium; the lowest (0.06±0.01 g L^{-1} day^{-1}) and highest (0.24±0.04 g L^{-1} day^{-1}) values were obtained in ASW under LL and HL, respectively (Fig. 4). Average TFA productivity under HL declined by 30 % as compared to the value of 0.34±0.04 g L^{-1} day^{-1} obtained under the same culture conditions (ASW) but with 30 % less (1.0 g L$^{-1)}$ potassium nitrate in the medium (Pal

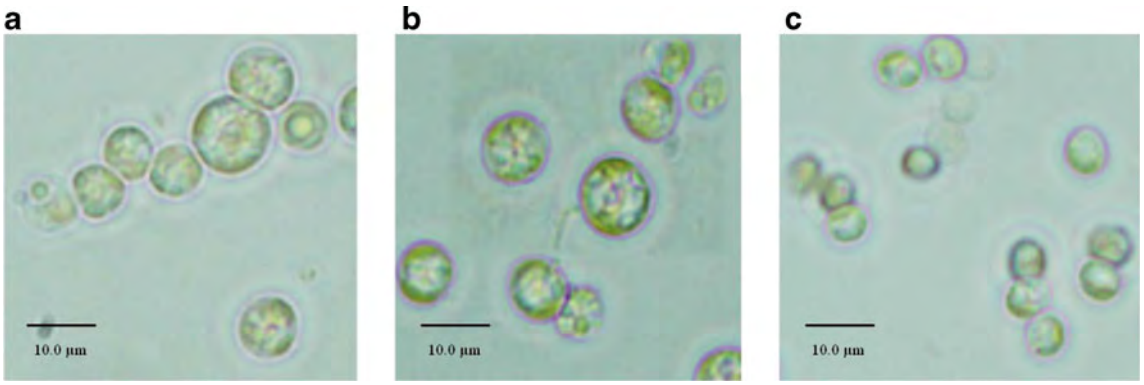

Fig. 1 Light micrograph of *N. oceanica* CCALA 804 cells cultivated in three nutrient media: **a** mBG-11, **b** SFM, and **c** ASW

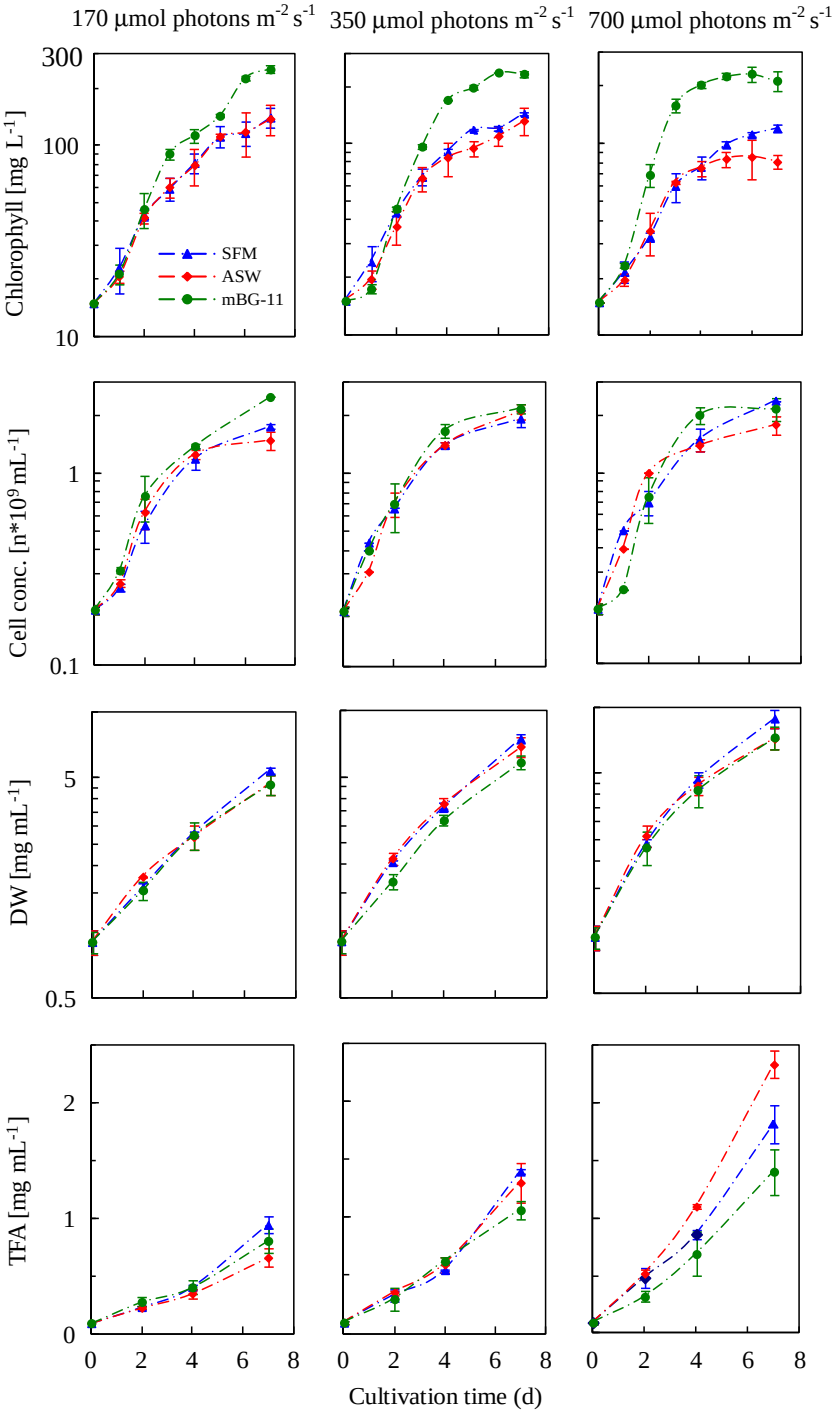

Fig. 2 Effect of irradiance level on chlorophyll a content, cell concentration, DW, and total fatty acid (TFA) volumetric content in *N. oceanica* CCALA 804 cultures grown in the different nutrient media: *diamond* ASW (27 g L^{-1} NaCl), *triangle* SFM (no NaCl), *circle* mBG-11. *Error bars* represent SD

et al. 2011). This might be explained by the slower depletion of the nitrogen source from the medium, affecting the intercellular C/N ratio and thus slowing the TAG accumulation occurring in the stationary cultures (Pal et al. 2011). The highest average TFA productivity achieved in SFM under LL and ML was associated with the highest biomass productivity. In contrast, the highest biomass culture content (Fig. 2) and average biomass productivity (Fig. 4) determined in SFM under HL were not accompanied by enhanced FA production, indicating the prevalent production of cell components other than storage lipids, e.g., proteins, membrane lipids, or carbohydrates.

Effects of osmotic downshift on biomass FA composition and content

In general, the TFA content of the biomass (in percentage of DW) was higher at higher PAR levels. The most substantial

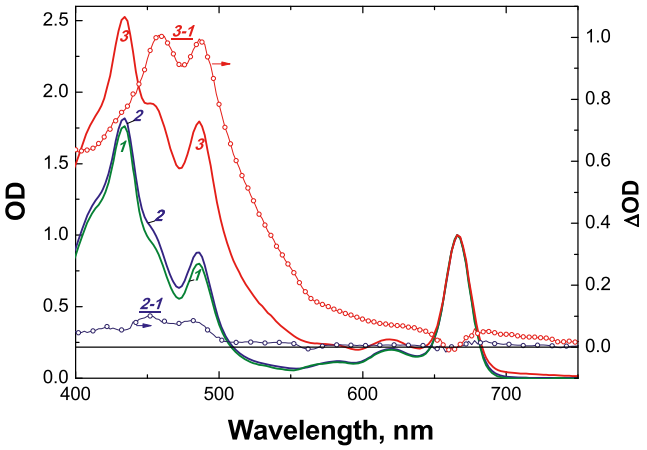

Fig. 3 Absorbance spectra of DMSO extracts of *N. oceanica* CCALA 804 cells grown at 170 μmol photon m^{-2} s^{-1} at inoculation (*1*), 7 days after osmotic downshift (*2*) and under continuous cultivation in ASW medium (*3*), as well as the corresponding difference spectra (*2–1* and *3–1*; *right* scale). Spectra *1–3* are normalized to the red chlorophyll absorption maximum

increase (from 9.5 % on day 0) was shown by the cultures in ASW, reaching a maximum 32 % of DW under HL on day 7 (Table 1). Notably, the biomass and per-cell TFA contents were less affected by PAR in SFM and mBG-11 (Tables 1, 2; Fig. S2). Two days after the medium change under LL, the proportion of 16:0 decreased substantially, with a concomitant rise in the proportion of EPA, in the FA profile of the cells grown in mBG-11 and ASW. However, following the transfer to SFM, the relative proportion of the saturated FA 16:0 did not change as compared to the culture at time 0, whereas the percentage of EPA increased concomitantly with a cumulative decrease in the relative proportions of several less abundant FAs, including 14:0, 18:1, 18:3 n-6, and 20:4 n-6 (Table 1). The effects of HL on the FA profile comprised an increase in the proportion of 16:0 with a concomitant decline in the major LC-PUFA 20:5 n-3 (EPA) in the cultures grown in the three media. In line with the higher Chl *a* content, implying increased content of EPA-rich chloroplast lipids (Sukenik et al. 1993b; Sukenik 1999), the biomass in mBG-11 retained a higher proportion of EPA out of TFA in the stationary phase as compared to ASW and SFM. Notably, a rise in the proportion of 16:0, characteristic of the storage lipid class TAG (Pal et al. 2011), was recorded only on day 7 in the cultures grown in mBG-11 under HL, in accordance with the delay in Chl *a* and EPA decline in this medium. A modest increase in 18:1 was evident in the cells grown in SFM under LL and in ASW under ML and HL on day 7. In the FA profile of the stationary cells under ML and HL, the increased proportion of 18:1 was accompanied by a decrease in the proportions of 18:2 n-6, arachidonic acid (ARA, 20:4 n-6, an immediate precursor of EPA), and EPA. Regardless of irradiance, the FA profile of the cells grown in mBG-11 also featured a higher percentage of ARA with a decrease in the proportion of the shorter-chain saturated FA 14:0 and 16:0.

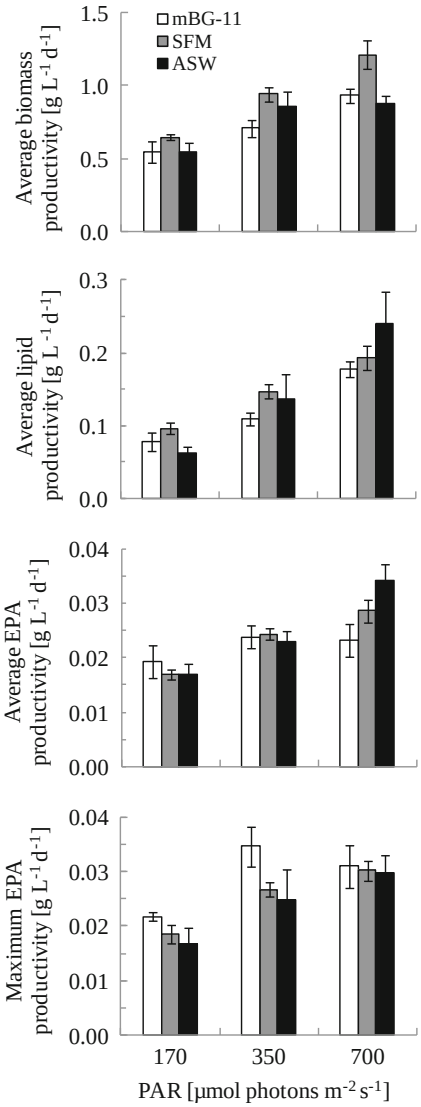

Fig. 4 Effect of irradiance and medium composition on average biomass and lipid TFA, and average and maximum EPA productivity by *N. oceanica* CCALA 804 grown in different media. *White bars*, mBG-11; *gray bars*, SFM (no NaCl); *black bars*, ASW (27 g L^{-1} NaCl). *Error bars* represent SD

The highest EPA percentage was found in cells in the late-log phase, reaching a maximum of *ca*. 30 % of TFA under LL and ML on day 4 in mBG-11. The maximum EPA content (5.7 % of DW) was obtained in mBG-11 under ML at the end of the log phase, with a maximum average EPA productivity of *ca*. 34 mg L^{-1} day^{-1} (for the 4-day growth period; Fig. 4). Under ML conditions, a sharp increase in the EPA percentage of TFA was accompanied by increased TFA content of the biomass, while the average biomass productivity was not different from other treatments, justifying the highest maximal EPA productivity. The EPA percentage of TFA and biomass decreased as the culture aged, most markedly under HL (Table 2), probably due to galactolipid turnover under these conditions (Fisher et al. 1998) and TAG accumulation

Table 1 Fatty acid composition and biomass content of EPA and total fatty acids (TFA) in *N. oceanica* CCALA 804 cells cultivated in SFM and ASW under different PAR

PAR (μmol m^{-2} s^{-1})	Time (days)	Medium	Fatty acid composition (% of TFA)[a]									EPA (% DW)	TFA (% DW)
			14:0	16:0	16:1[b]	18:1 n-9	18:2 n-6	18:3 n-6	18:3 n-3	20:4 n-6	20:5 n-3		
	0		6.3	30.0	26.3	3.1	3.2	0.7	0.2	4.2	20.6	2.1±0.3	9.5±2.2
170	2	SFM	5.2	29.1	26.1	2.3	4.3	0.5	0.2	3.7	24.5	3.6±0.1	14.6±0.4
		ASW	7.1	26.9	25.5	2.7	4.2	0.5	0.3	4.8	24.7	3.1±0.2	12.7±1.0
	4	SFM	5.2	28.5	25.8	3.5	5.1	0.3	0.2	4.3	23.6	3.4±0.2	14.5±1.0
		ASW	6.6	21.2	24.7	3.3	4.9	0.4	0.2	5.4	28.2	3.7±0.3	13.0±1.1
	7	SFM	4.6	33.5	24.9	7.5	4.2	0.3	tr	3.6	17.9	3.1±0.1	17.5±1.3
		ASW	6.7	24.8	26.7	4.5	4.3	0.4	0.2	4.0	24.6	3.5±0.2	13.9±0.4
350	2	SFM	5.0	33.0	26.2	3.2	3.5	0.5	0.2	3.6	21.0	3.4±0.6	16.0±0.8
		ASW	6.0	36.7	26.5	3.9	2.7	0.6	0.2	3.6	17.4	3.1±0.4	16.5±1.8
	4	SFM	5.1	30.6	25.8	4.4	3.9	0.3	0.2	3.6	23.0	3.4±0.1	15.0±0.5
		ASW	6.0	29.6	27.2	6.1	2.6	0.3	tr	3.0	22.3	3.5±0.3	15.6±1.2
	7	SFM	4.6	35.6	24.6	8.5	3.2	0.2	tr	3.2	17.0	3.2±0.3	18.7±0.4
		ASW	5.9	31.0	26.1	9.6	1.8	0.3	tr	2.4	19.6	3.7±0.4	20.3±1.9
700	2	SFM	4.8	36.9	25.7	5.5	2.7	0.7	0.2	3.2	15.5	2.2±0.8	19.8±3.5
		ASW	5.6	39.3	26.3	4.6	1.8	0.4	tr	2.8	15.6	3.0±0.2	19.5±1.2
	4	SFM	5.1	35.8	25.6	6.4	3.1	0.3	0.2	3.0	17.7	3.3±0.3	19.2±1.2
		ASW	5.8	36.0	26.2	9.6	1.6	0.3	tr	1.7	16.4	3.9±0.1	23.9±0.3
	7	SFM	4.4	36.3	26.0	8.9	3.0	0.3	tr	2.7	15.3	3.1±0.4	20.4±1.1
		ASW	5.6	36.1	26.6	12.6	1.5	0.4	0.2	1.6	13.7	4.5±0.3	32.2±2.6

Data are means of $n=3–4$. Presented data are mean values with a range of less than 5 % for major sample peaks (over 10 % fatty acids) and 10 % for minor sample peaks, each analyzed in duplicate

tr trace

[a] 20:0, 20:2 n-6, 20:3 n-6, and 22:0 were present at less than 1 %

[b] Total of 16:1 isomers, the predominant isomer being 16:1 n-7

Table 2 Major fatty acid composition and biomass content of EPA and total fatty acids (TFA) of *N. oceanica* CCALA 804 cultivated in mBG-11 under different PAR

PAR (μmol m^{-2} s^{-1})	Time (days)	Fatty acid composition (% of TFA)[a]										EPA (% DW)	TFA (% DW)
		14:0	16:0	16:1[b]	18:0	18:1 n-9	18:2 n-6	18:3 n-6	18:3 n-3	20:4 n-6	20:5 n-3		
	0	6.6	29.4	27.5	1.1	3.1	3.0	0.8	tr	4.4	20.2	1.6±0.6	7.7±2.0
170	2	5.1	22.4	26.2	0.8	4.0	3.7	0.5	0.2	4.1	22.1	4.1±0.2	14.2±0.1
	4	5.7	21.9	27.8	0.6	2.0	4.4	0.4	0.2	4.4	30.1	4.3±0.4	14.4±0.6
	7	5.6	25.6	25.6	0.5	3.8	4.7	0.5	0.3	4.8	24.4	4.1±0.1	16.8±1.4
350	2	4.7	29.1	26.8	0.7	4.7	2.9	0.5	0.2	4.3	22.7	3.2±0.1	14.0±0.3
	4	5.4	21.4	28.0	0.4	2.4	4.4	0.4	0.2	4.7	29.7	5.7±0.1	19.2±0.2
	7	5.9	27.5	25.1	0.5	3.8	4.4	0.3	0.2	4.9	23.3	5.2±0.1	21.5±2.2
700	2	5.1	26.2	28.0	0.5	3.2	3.4	0.5	0.3	4.4	26.5	2.9±0.7	11.6±3.4
	4	6.4	27.4	27.0	0.4	2.5	4.6	0.3	tr	5.0	26.8	3.7±0.4	14.9±2.5
	7	5.9	35.0	24.7	0.7	7.6	3.8	0.2	tr	4.5	17.0	3.2±0.3	21.8±3.1

[a] 20:0, 20:2 n-6, 20:3 n-6, and 22:0 were present at less than 1 %

[b] Total of 16:1 isomers, the predominant isomer being 16:1 n-7

Data are means (n=3–4). Presented data are mean values with a range of less than 5% for major sample peaks (over 10% fatty acids) and 10% for minor sample peaks, each analyzed in duplicate.

(Pal et al. 2011), whereas the average EPA productivity (for the 7-day growth period) under HL reached its highest value in ASW due to the highest average TFA productivity (Fig. 4). Note that in the absence of NaCl (SFM), the average EPA productivity increased with the increase in PAR from LL to HL, and was not significantly different from that in ASW under LL and ML, while demonstrating lower values under HL (Fig. 4). Hence, both the average TFA productivity and EPA percentage of TFA and biomass contributed to the average and maximal EPA productivity of *N. oceanica* CCALA 804 cultures.

Effects of osmotic downshift on the distribution of individual lipid classes and their FA composition

To elucidate the alterations in the distribution of lipid classes and their FA composition following osmotic downshift, we analyzed FA composition and content of the major chloroplastic and extraplastidial lipids 2 and 4 days after transfer from ASW to SFM under LL. We assumed that under LL, the effect of the osmotic downshift on lipid class distribution would not be masked by the effect of increasing light intensity on storage lipid formation. The results obtained for day 4 demonstrated essentially the same pattern of change as those for day 2 and are therefore not shown. Due to the different macro- and micronutrient compositions of mBG-11, which might have multiple effects, in this work we did not perform analysis of lipid class distribution under these conditions.

After the transfer to SFM, acyl lipid distribution showed a substantial increase in the relative proportion of the major chloroplast galactolipid monogalactosyldiacylglycerol (MGDG; from 12.6±0.1 to 20.0±2.4 of total acyl lipids; Fig. 5). The proportion of the second major galactolipid digalactosyldiacylglycerol (DGDG) remained unaltered; hence, a twofold increase in the MGDG/DGDG ratio was determined compared to cells grown in ASW. The increase in the proportion of MGDG occurred on the background of a decreasing proportion of TAG, along with some decline in the acidic chloroplast lipid sulfoquinovosyldiacylglycerol (SQDG). The proportions of two major extraplastidial lipids, phosphatidylcholine (PC) and the betaine lipid diacylglyceryl-*N*,*N*,*N*-trimethylhomoserine (DGTS), were not affected, whereas that of phosphatidylethanolamine (PE) increased from 2.8±0.28 to 4.4±0.42. It is important to note that these alterations were accompanied by an increase in the TFA content of the biomass and culture relative to time 0 (Table 1) accompanied by cell division, suggesting that de novo production of acyl lipids is largely responsible for the increased share of MGDG and PE.

Among the chloroplast membrane lipids, only the FA composition of DGDG demonstrated substantial changes upon osmotic downshift, namely a decreased proportion of EPA with a concomitant increase in 16:1. FA compositions of

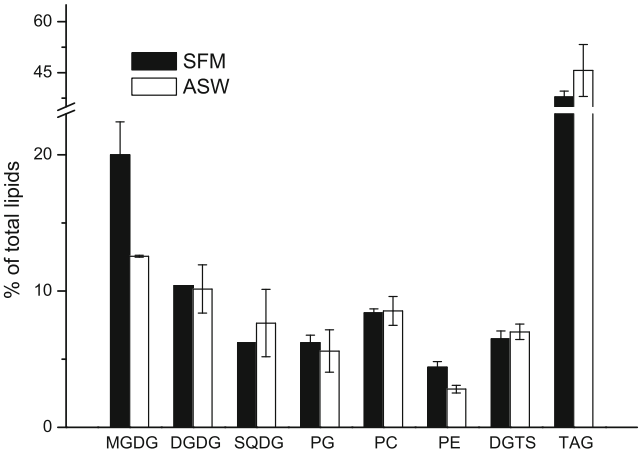

Fig. 5 Effect of the osmotic downshift (2 days after transfer from ASW to SFM) on the proportions of individual lipid classes in total acyl lipids of *N. oceanica* CCALA 804 grown at a PAR of 170 μmol photon m^{-2} s^{-1}

MGDG, SQDG, and phosphatidylglycerol (PG) were not substantially affected (Table 3). Both MGDG and PG were highly enriched in EPA, whereas 14:0 and 16:1 were more abundant in MGDG. PG contained 16:1Δ3 *trans* isomer, comprising 2.2 and 2.8 % of the TFA in SFM- and ASW-grown cultures, respectively. DGTS had the highest proportion of EPA (up to *ca*. 65 %) among the extraplastidial membrane acyl lipids (Table 3). The EPA proportion in the FA of DGTS declined with culture age (not shown); this decline was more pronounced in the cells transferred to SFM than in those grown in ASW and was accompanied by an increase in the proportions of 16:0, 18:1, 18:2, and ARA. Upon transfer to SFM, the FA profile of PC changed mainly in the proportions of C18 FA rather than of LC-PUFA. This phospholipid featured the highest abundance of 18:1 n-9 and 18:2 n-6 among the polar lipids and their ratio changed notably due to a sharp decrease in the proportion of 18:1 n-9 in SFM, with a concomitant increase in 16:1. The FA profile of PE showed the most substantial change: a significant decrease in the proportion of ARA with a concomitant increase in those of EPA and 16:1 (Table 3). The minute changes in the FA composition of TAG in SFM included some increases in the percentages of 16:0 and 18:2 n-6 (Table 3); EPA comprised *ca*. 3 % of the TFA in TAG. Free fatty acids comprised a minor fraction and were enriched in EPA (not shown).

Metabolic adjustments of *N. oceanica* CCALA 804 upon osmotic downshift

The GC–MS-based metabolite profile of *N. oceanica* CCALA 804 cells grown in ASW and SFM comprised over 50 identified metabolites (GMD, http://gmd.mpimp-golm.mpg.de/), several of them showing a differential response to osmotic downshift (Figs. 6 and 7). Particularly, a significantly higher

Table 3 Fatty acid composition of major lipid classes in *Nannochloropsis* sp. *oceanica* CCALA 804 in ASW and 2 days after transfer to SFM (under 170 μmol photon m^{-2} s^{-1})

Fatty acids	MGDG		DGDG		SQDG		PG		PC		PE		DGTS		TAG	
	SFM	ASW	SFM	ASW	SFM	ASW	SFM	ASW	SFM	ASW	SFM	ASW	SFM	ASW	SFM	ASW
14:0	10.9±0.1	12.8±0.2	5.5±0.0	6.3±0.1	4.6±0.4	5.0±0.3	1.0±0.1	1.0±0.1	1.6±0.2	1.9±0.1	1.5±0.1	1.5±0.3	2.3±0.2	3.1±0.6	6.1±0.6	7.4±0.1
16:0	13.9±1.0	14.5±0.9	31.4±0.9	29.9±0.6	47.0±3.4	45.2±4.4	39.1±0.9	39.8±0.7	20.4±0.5	20.5±1.6	8.0±2.7	5.3±1.0	8.1±0.4	7.2±0.9	46.7±1.0	44.1±0.8
16:1[a]	12.4±0.3	10.6±1.9	28.2±1.5	23.6±1.2	39.2±1.8	37.7±1.9	6.6±0.4	6.9±0.1	28.2±3.8	24.2±0.7	18.9±2.0	13.8±2.5	12.5±0.1	11.8±1.3	33.6±1.7	36.2±1.0
18:0	0.3±0.1	0.4±0.2	0.3±0.1	0.3±0.1	0.5±0.1	0.8±0.0	0.3±0.1	0.5±0.0	0.3±0.1	0.5±0.1	0.9±0.0	0.8±0.1	0.5±0.2	0.5±0.0	1.2±0.1	1.2±0.1
18:1 n-9	0.6±0.3	0.8±0.6	0.7±0.1	0.7±0.2	1.0±0.4	1.6±0.7	0.8±0.3	1.0±0.0	7.2±0.4	13.1±3.8	2.1±0.1	3.7±0.5	0.8±0.2	1.1±0.0	3.6±0.7	4.1±0.5
18:2	1.3±0.2	1.2±0.3	2.0±0.4	1.5±0.2	1.9±1.5	2.2±1.7	1.5±0.5	0.9±0.0	22.1±0.4	18.9±1.4	4.8±0.1	4.1±0.6	2.4±0.2	2.0±0.2	2.5±0.1	1.8±0.0
18:3 n-6	0.2±0.0	0.2±0.1	0.1±0.0	0.1±0.0	0.2±0.1	0.3±0.2	0.1±0.1	0.0±0.0	1.2±0.3	1.3±0.5	1.5±0.1	1.2±0.1	0.3±0.0	0.3±0.0	0.1±0.0	0.1±0.1
18:3 n-3	0.1±0.1	0.1±0.1	0.2±0.0	0.1±0.0	0.1±0.1	0.1±0.1	0.1±0.0	0.0±0.1	0.4±0.0	0.3±0.0	0.3±0.1	0.0±0.0	0.3±0.1	0.2±0.0	0.1±0.1	0.0±0.0
20:4 n-6	2.5±0.6	2.4±0.2	0.7±0.1	1.3±0.8	1.4±0.7	1.7±1.0	1.6±0.3	1.8±0.0	5.0±1.5	6.9±1.9	23.0±1.3	35.7±1.1	6.6±0.7	7.3±1.3	0.7±0.0	0.6±0.0
20:5 n-3	56.6±2.3	55.8±4.7	29.9±0.6	35.2±2.5	3.2±1.6	3.7±1.9	44.8±1.8	43.8±0.3	9.0±1.2	8.5±0.7	33.1±0.9	28.6±2.9	64.2±1.4	64.9±2.0	2.8±0.6	2.8±0.2

[a] Total of 16:1 isomers, the predominant isomer being 16:1 n-7

abundance ($p<0.05$) of the largest chromatographic peak as compared to the cells transferred to SFM was revealed. The closest annotation match for this peak in the GC–MS library was determined to be either sorbitol or mannitol. By using a split method (1:32) of GC–MS injection instead of a splitless mode (see "Materials and methods" section) and spiking with either a sorbitol or mannitol standard prior to derivatization, mannitol was detected as the major polyol in *N. oceanica* CCALA 804 cells (Fig. S3). As shown in Fig. 6, the relative abundance of mannitol decreased significantly (to *ca*. 40–50 % that in ASW, $p<0.05$) following osmotic downshift (2 days after the transfer) under both PAR levels. Note that a lower mannitol level was also found in the cells grown under HL as compared to LL in SFM. The ability to produce mannitol was further supported by a BLAST similarity search (http://blast.ncbi.nlm.nih.gov) of available genomic data for *Nannochloropsis* species using a higher plant (*Apium graveolens*) mannose 6-phosphate reductase (Zhifang and Loescher 2003) (GenBank accession no. AAB9761) as a hit. In the genome of *N. gaditana* CCMP526, the search revealed a putative mannose 6-phosphate reductase (accession no. AFJ69400; 46 % identity), essential for mannitol biosynthesis, as well as a putative mannitol 1-phosphate dehydrogenase (accession no. AFJ69261.1) required for mannitol degradation.

Figure 7 shows other identified metabolites with significantly changed content ($p<0.05$) after osmotic downshift under LL and HL. Spermidine was among the predominant metabolites whose relative content decreased *ca*. one order of magnitude upon transfer to SFM under both PAR levels. The decrease was more pronounced under the less stressful conditions of LL, indicating that light intensity contributes to the change in content. Similarly, the relative content of proline was significantly higher in ASW vs. SFM (fivefold increase), particularly under HL, revealing the importance of this compatible solute for adaptation of *N. oceanica* CCALA 804 to a saline environment. The decrease in proline in SFM was associated with increases in its precursors in the delta1-pyrroline-5-carboxylate-proline cycle (Miller et al. 2009) — glutamate, the related pyroglutamate (5-oxoproline) and arginine—supporting the evidence of decreased proline biosynthesis under hypotonic conditions. The level of glutamate's metabolic product γ-aminobutyric acid (GABA) increased over twofold in SFM in a light-dependent manner, suggesting GABA's involvement in algal cell adjustment to low salinity, particularly when the osmotic downshift is combined with HL.

Glucose 6-phosphate (Glu-6-P), glycerophosphoglycerol (GPG), and inositol 3-phosphate showed a similar decreasing pattern following osmotic downshift. The decrease in the central cellular metabolite Glu-6-P (up to *ca*. 40 and 30 % of its relative content in ASW under LL and HL, respectively) displayed a light-dependent pattern upon transfer to SFM, suggesting increased glycolytic flux toward osmoprotectant

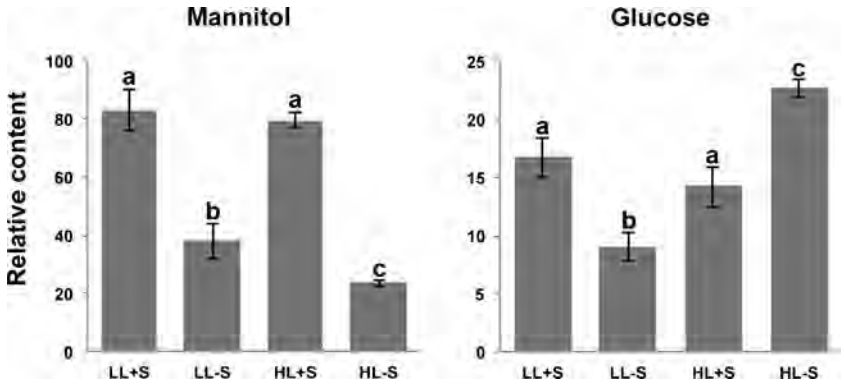

Fig. 6 Relative content (*Y*-axis) of mannitol and glucose, determined on day 2 after osmotic downshift, under LL and HL. *Bars* represent means±SD (n=6). Different *lowercase letters* represent significant changes according to *t* test of significance with confidence interval of 95 %. ASW is designated as [+S], SFM as [−S]

formation under higher osmolarity. Indeed, under HL, the relative content of glucose increased twofold in SFM on the background of the prominent decrease in Glu-6-P (Figs. 6 and 7).

The relative abundance of GPG, a deacylation product of PG and, perhaps, a phosphorylated form of glycerol-3-phosphate (G-3-P), decreased in SFM with a concomitant increase in the relative content of G-3-P, indicating the substrate-to-product conversion.

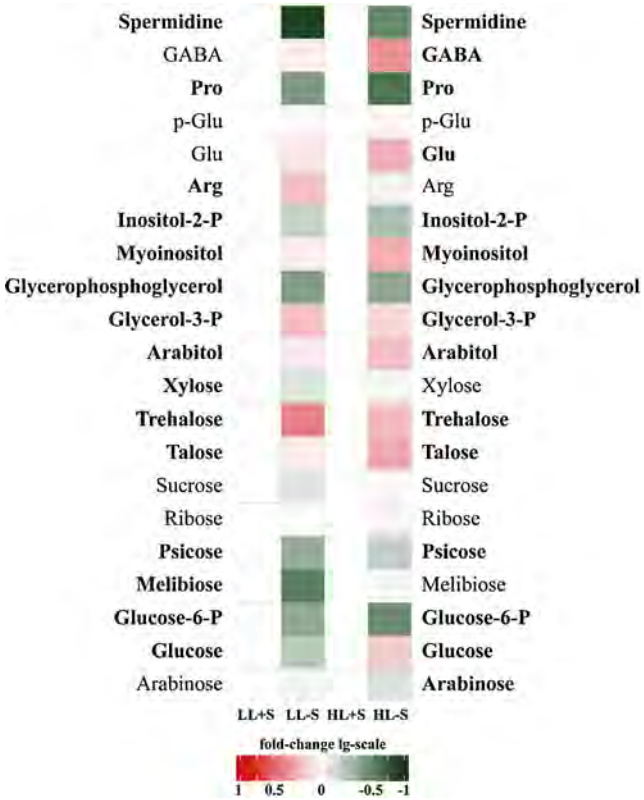

Fig. 7 Heatmap of the relative contents of the metabolites identified by GC–MS analysis. Each value of each metabolite was divided by its own control (ASW, +S), and log10-transformed. Cells represent means (n=6, for HL-S n=3). Metabolites in *bold* changed significantly in SFM (−S) compared to their own control ASW (+S), according to *t* test with confidence interval of 95 % and assumed equal variance. *Pro* proline, *p-Glu* pyroglutamate, *Glu* glutamate, *Arg* arginine, *P* phosphate

The relative contents of monosaccharides, such as the pentose arabinose, decreased in SFM, especially under HL, whereas the pentitol arabitol, derived from arabinose, increased in the same light-dependent manner (Fig. 7). A similar decreasing pattern was found for the 5-C monosaccharide xylose and the disaccharide sucrose; the 6-C monosaccharide psicose decreased more sharply (to 40 and 60 % of its relative content in ASW under LL and HL, respectively) than other monosaccharides, while the relative content of glucose declined only under LL (Fig. 6). Melibiose, a disaccharide of galactose and glucose, decreased significantly (up to 20 % of its relative content in ASW) under LL upon transfer to hypotonic conditions, suggesting its osmoprotective role in saline medium. It is also likely that galactose, which showed less conversion to melibiose in SFM, can be utilized for biosynthesis of the galactolipid MGDG (Fig. 5). Notably, glucose, followed by mannose and trace amounts of rhamnose, fucose, arabinose, xylose, and galactose, have been determined in polysaccharides and cell wall components of *N. oceanica* CCMP1779 (Vieler et al. 2012). An increasing trend following osmotic downshift was observed for the stress-related disaccharide trehalose (threefold increase under LL) and the aldohexose talose (twofold increase under HL).

Discussion

Tolerance to variations in osmotic pressure and ionic concentrations, described in several euryhaline microalgae (Brown and Hellebust 1980; Brown 1982; Kirst 1989), is a prerequisite to and an important ecological consequence of successful competition and survival in habitats characterized by variable osmotic conditions. The tolerance to sudden hypotonic stress is also essential for sustainable biomass production outdoors in open shallow ponds that are exposed to precipitation events. On the other hand, medium evaporation and the subsequent rise in salt concentration is a frequently occurring event in outdoor microalgal cultivation facilities in countries with warm climates, which may

negatively affect culture productivity. It seems that the limits of salinity tolerance of *N. oceanica* CCALA 804 (earlier designated *Nannochloropsis* sp.) are dependent on nitrate source availability (Pal et al. 2011). Nitrogen-replete cultures were able to withstand the NaCl concentration of 40 g L^{-1} at a PAR of 700 μmol m^{-2} s^{-1}, demonstrating high biomass and TFA productivities, whereas increasing NaCl to 40 g L^{-1} in nitrogen-depleted cultures was detrimental to biomass and TFA production. In our previous work, a positive relationship between a decrease in NaCl concentration below 27 g L^{-1} and an increase in biomass and EPA proportion of TFA by nitrogen-replete cultures was demonstrated (Pal et al. 2011). Thus, the major focus of the current work was a deeper elucidation, at the physiological and biochemical levels, of the obvious plasticity of *N. oceanica* CCALA 804 metabolism in response to drastic osmotic downshift.

Our results demonstrate that *N. oceanica* CCALA 804 grown in nitrogen-replete media under laboratory conditions tolerates drastic osmotic downshifts. Shifting the cells from ASW to freshwater media did not cause cell rupture (Fig. 1) or a prolonged lag in cell divisions or biomass production; in fact, the biomass productivity increased in SFM (Fig. 5). It is important to state that the higher growth rate in mBG-11, resulting in the highest Chl *a* contents, EPA percentage and productivity (Figs. 2 and 4 and Table 2), emphasizes the importance of micro- and macronutrient composition of the nutrient medium, apart from salinity, for optimal EPA production by *Nannochloropsis* microalgae; it also pinpoints the importance of further medium optimization. The growth- and photosynthesis-promoting effects of osmotic downshifting have been described in some marine chlorophytes, e.g., *Nannochloris bacillaris* Naumann (Brown 1982). Similarly, in *Nannochloris coccoides*, growth rate, chlorophyll content, light-saturated photosynthetic capacity, light-harvesting efficiency, and respiration were enhanced by a decrease in salinity from 150 to 0 TDS units (Henley et al. 2002). We suggest that the enhanced biomass productivity of *N. oceanica* CCALA 804 cultured in SFM, especially under higher PAR, is associated with adjustments of the pigment apparatus and chloroplast lipid composition; these adjustments likely enhance photosynthetic efficiency, and facilitate photosynthetic carbon fixation and photoassimilate allocation to simple carbohydrates, proteins, and structural lipid biosynthesis, rather than to the production of compatible solutes and lipid reserves (Figs. 5, 6, and 7). This suggestion is supported by the higher Chl *a* content (Fig. 2) of *N. oceanica* CCALA 804 cells grown in SFM and mBG-11 vs. ASW. The Car/Chl *a* ratio, a sensitive marker of stress in microalgae, including *Nannochloropsis* (Solovchenko et al. 2011), tended to decline after transfer to media lacking NaCl, suggesting that the osmotic downshift does not trigger a pronounced stress response in the *N. oceanica* CCALA 804 pigment apparatus (*cf.* curves 1 and 2 in Fig. 3). Conversely, in the cells grown in ASW, the stress-related pathways of osmolyte and reserve lipid biosynthesis were induced. Accordingly, an increase in PAR readily leads to higher TFA accumulation and average TFA productivity. Hence, the cultures grown in ASW demonstrated higher average TFA productivity under HL, but the values were still lower than in the previous study because of a higher initial nitrate concentration.

We previously reported enhanced growth and EPA content in parallel with a decrease in TFA content upon lowering salinity (NaCl) to 50 % of that in ASW (Pal et al. 2011), indicating the prevalent formation of chloroplast membrane lipids rich in EPA over the storage TAG. In the present work, we investigated the ability of *N. oceanica* CCALA 804 to adjust FA composition of individual lipids and modify acyl lipid class distribution in response to hypotonic challenge. Here, we studied alterations in lipid composition under low PAR with the assumption that changes characteristic of the osmotic downshift would be less masked by the enhanced production of neutral lipids occurring under high PAR (Pal et al. 2011). Among the strategies evolved by phytoplanktonic microalgae to survive in surface-water layers, the ability to rapidly adjust cellular lipid metabolism and swiftly modify the distribution and degree of unsaturation of membrane lipids might play an important role. In particular, the content of chloroplast lipids often decreases under high salinity stress (Guschina and Harwood 2009).

A detailed analysis of acyl lipid composition in *Nannochloropsis* sp. has been previously performed, and the EPA biosynthesis pathway has been elucidated by radiolabeling studies (Schneider and Roessler 1994; Sukenik 1999) and more recently confirmed by genome annotation of two *Nannochloropsis* species (Vieler et al. 2012; Jinkerson et al. 2013). The terminal Δ17 (omega-3) lipid-linked desaturation of ARA to EPA was proposed to occur in PE. However, to the best of our knowledge, this desaturase has not been cloned or functionally confirmed. Highly unsaturated MGDG and DGTS of *Nanochloropsis*, featuring more that 50 % of EPA of their acyl moieties (Table 3), contain molecular species with EPA occupying both positions on the glycerol backbone. Less unsaturated DGDG contains about 30 % of EPA within molecular species, represented by combinations of EPA with either 16:0 or 16:1. The shift to SFM affected the FA composition of DGDG most noticeably, decreasing its unsaturation level by decreasing EPA percentage with a corresponding increase in 16:1.

The major modification in the distribution of acyl lipid classes seemed to be the higher relative proportion of the bilayer-destabilizing lipid MGDG (Fig. 5) and the consequent twofold rise in the MGDG/DGDG ratio, accompanied by an increase in the cell and culture contents of Chl *a* (Fig. 2, Fig. S2). The observed lower MGDG/DGDG ratio in ASW is in line with previously documented galactolipid modifications, for instance those occurring in the freshwater cyanobacteria *Synechococcus* (Huflejt et al. 1990) and in

algae of different classes at higher salinities (Stefanov et al. 1994 ; Stefanov et al. 1994). Since DGDG is synthesized from MGDG (Dörmann and Benning 2002), a plausible interpretation is that with increasing MGDG biosynthesis, less MGDG molecular species (20:5/16:0 and 20:5/16:1) (Sukenik et al. 1993a) of *Nannochloropsis* cells are available for DGDG biosynthesis. The altered ratio of the major galactolipids induces substantial changes in the physicochemical properties of the chloroplast envelope and thylakoid membranes, since MGDG is a non-bilayer lipid forming a Hex-II phase, whereas DGDG is a bilayer-forming lipid (Jarvis et al. 2000; Dörmann and Benning 2002; Aronsson 2008). In contrast to ASW, in the absence of NaCl, the increased proportion of MGDG may result in membrane destabilization, thus affecting fluidity and permeability the structural organization of the thylakoids and integral membrane protein function. It thus appears that *N. oceanica* CCALA 804 undergoes only slight adjustments in the FA composition of its chloroplast lipids to tolerate hypotonic conditions, whereas more pronounced alterations occur in the phospholipids, which are suggested to be the sites of sequential lipid-linked desaturations leading to EPA production prior to its import by the chloroplast (Schneider and Roessler 1994; Sukenik 1999). In addition, the effect of osmotic downshift on plasma membrane lipid composition cannot be excluded, given the increased surface area of the cells in SFM and mBG-11.

Metabolite profiling by GC–MS clearly revealed the decreased production of several compatible solutes, such as the major polyol mannitol and the amino acid proline. We identified mannitol as the major polyol in *N. oceanica* CCALA 804 and showed that its production is enhanced at higher NaCl levels. The ability to increase mannitol content with increasing salinity was previously described as a strategy to adjust cellular metabolism in two euryhaline eustigmatophytes (Brown and Hellebust 1980). In line with these data, the freshwater isolate of *Ectocarpus* (brown algae) was characterized by lower intracellular mannitol concentrations as compared to a strictly marine strain of *Ectocarpus siliculosus* (Dittami et al. 2012). Furthermore, the freshwater strain demonstrated extremely low expression of the mannitol 1-phosphate dehydrogenase gene. In addition, increased mannitol production has been shown to protect *Saccharomyces cerevisiae* from oxidative stress (Chaturvedi et al. 1997). Thus, apart from playing a role in osmoregulation, mannitol may function in protecting cells from reactive oxygen species production, particularly under the stressful conditions of high salinity and HL.

The reduced content of the stress-responsive polyamine spermidine, playing a pivotal role in plant cell defense against environmental stresses (Alcázar et al. 2010), in the cells in SFM could be attributed to the decreased activity of spermidine synthase (Kasukabe et al. 2004). Proline biosynthesis is reduced under hypotonic conditions, an additional indication of the relief from osmotic stress. Our results suggest that more glutamate accumulates and likely becomes diverted to GABA biosynthesis mediated by glutamate decarboxylase. These results are to some extent unexpected due to the often suggested involvement of GABA in the osmotic stress response (Fait et al. 2008). A more plausible explanation for the role of GABA accumulation following osmotic downshift is in the GABA shunt representing a major route for C–N repartitioning and Glu recycling (reviewed in Fait et al. 2008). The increase in GABA (almost threefold) under HL in SFM is in line with regulation of the GABA shunt by reactive oxygen intermediates as shown in other studies (Busch and Fromm 1999; Bouché et al. 2003; Fait et al. 2005).

G-3-P increased while glycerol-rich GPG decreased following osmotic downshift. A possible interpretation is that under higher osmolarity, G-3-P, and probably GPG are converted to glycerol by glycerol 3-phosphatase, whereas following osmotic downshift, excess glycerol might be removed by the activity of glycerol kinase on glycerol and GPG, thus producing G-3-P. The latter can be utilized for the membrane lipid and TAG biosynthesis induced by transfer to HL. GPG has been identified in the acidic polyphosphate-rich vacuoles of the halotolerant microalga *Dunaliella salina* which accumulates glycerol as a major compatible solute (Ginzburg et al. 1988). This suggests that accumulation of this metabolite under conditions of osmotic stress might serve as a source for G-3-P production when growth conditions recover.

Prominent decreases were found for Glu-6-P and myo-inositol phosphate following the osmotic downshift (Fig. 7). Depletion of the hexose phosphate pool in SFM might result from the decreased glycolytic flux. It is also possible that glycolysis fails to initiate, due to the impaired phosphorylation of hexoses, which requires ATP. Together, these two processes would lead to decreased Glu-6-P. Increased photosynthetic glucose production, particularly under HL, might also be responsible for the increased relative glucose content. Free myoinositol increased following transfer to SFM, more strongly under HL, showing the same trend as glucose. Given that myoinositol 1-phosphate and myoinositol are produced from Glu-6-P, and that this pathway is essential for the synthesis of various metabolites in halophytes (Ishitani et al. 2002), we can speculate that myoinositol phosphate is required to support growth in saline media.

The stress-responsive sugar trehalose (Fernandez et al. 2012) increased in SFM. Trehalose 6-phosphate acts as a signaling metabolite of sugar status in plants, but its level is very difficult to measure (Lunn et al. 2006); we can therefore speculate that the level of trehalose 6-phosphate increases in saline medium, while free trehalose is produced in SFM, similar to glucose and myoinositol from their phosphorylated forms. It should also be mentioned that trehalose has been shown to accumulate only under specific conditions,

suggesting that it may display functions other than that of being a compatible solute (Obata and Fernie 2012).

To summarize, in this report we identified several mechanisms that enable the cells of *N. oceanica* CCALA 804 to cope with and acclimate to the osmotic downshift. The first mechanism is related to the barrier properties of the cell walls, allowing the cells to withstand the increased turgor pressure and remain intact (Fig. 1). The second strategy involves the adjustment of membrane physico-chemical properties, such as the fluidity of chloroplast membranes, by promoting MGDG formation over that of DGDG (Fig. 5). The third explored mechanism is based on the differential decline in the content of osmolyte and several stress-response markers within the cells (Figs. 6 and 7), allowing for the allocation of photoassimilates to growth and maintenance of chloroplast functional performance. Differential regulation of gene expression at the transcriptome level should be considered and requires further investigation. Indeed, massive changes in gene-expression patterns have been shown in *Ectocarpus* strains isolated from marine and freshwater environments and exposed to different salinity levels (Dittami et al. 2012).

Nannochloropsis microalgae have been extensively exploited as candidate organisms for outdoor cultivation for EPA and biodiesel production due to their robustness and plasticity in the face of variable growth conditions (Pal et al. 2011; Simionato et al. 2011). The ability to thrive in a freshwater environment should be examined in the long term as this might extend their field of application and have valuable commercial implications for the utilization of *Nannochloropsis* in biotechnology and aquaculture, particularly for alga- and fish-growing facilities where low-cost marine water resources are remote or unavailable. The capacity to withstand drastic osmotic changes in open outdoor systems might be useful in eliminating predator organisms that are less tolerant to these types of stresses. Finally, the results of this work may be exploited in research devoted to metabolic engineering of microalgae for enhanced salt tolerance.

Acknowledgments This research was financially supported by the European Commission's Seventh Framework Program for Research and Technology Development (FP7), project GIAVAP, Grant No. 266401. DP and AB acknowledge support from the Albert Katz International School for Desert Studies at BGU. AS acknowledges partial financial support from the Ministry of Science and Education of the Russian Federation (contract no. 14.515.11.0026), Russian Foundation of Basic Research, and "Skolkovo" Scientific Fund.

References

Ahmad I, Hellebust JA (1984) Nitrogen metabolism of the marine microalga *Chlorella autotrophica*. Plant Physiol 76:658–663

Ahmad I, Hellebust JA (1986) The role of glycerol and inorganic ions in osmoregulatory responses of the euryhaline flagellate *Chlamydomonas pulsatilla* Wollenweber. Plant Physiol 82:406–410

Alcázar R, Altabella T, Marco F, Bortolotti C, Reymond M, Koncz C, Carrasco P, Tiburcio AF (2010) Polyamines: molecules with regulatory functions in plant abiotic stress tolerance. Planta 231:1237–1249

Andersen RA, Brett RW, Potter D (1998) Phylogeny of the Eustigmatophyceae based upon 18S rDNA, with emphasis on *Nannochloropsis*. Protist 149:61–74

Aronsson H (2008) The galactolipid monogalactosyldiacylglycerol (MGDG) contributes to photosynthesis-related processes in *Arabidopsis thaliana*. Plant Signal Behav 3:1093–1095

Bai B, Sikron N, Gendler T, Kazachkova Y, Barak S, Grafi G, Khozin-Goldberg I, Fait A (2012) Ecotypic variability in the metabolic response of seeds to diurnal hydration–dehydration cycles and its relationship to seed vigor. Plant Cell Physiol 53:38–52

Bisson MA, Kirst GO (1995) Osmotic acclimation and turgor pressure regulation in algae. Naturwissenschaften 82:461–471

Bouché N, Fait A, Bouchez D, Moller SG, Fromm H (2003) Mitochondrial succinic-semialdehyde dehydrogenase of the γ-aminobutyrate shunt is required to restrict levels of reactive oxygen intermediates in plants. Proc Natl Acad Sci USA 100:6843–6848

Boussiba S, Vonshak A, Cohen Z, Avissar Y, Richmond A (1987) Lipid and biomass production by the halotolerant microalga *Nannochloropsis salina*. Biomass 12:37–47

Brown LM (1982) Photosynthetic and growth responses to salinity in a marine isolate of *Nannochloris bacillaris* (*Chlorophyceae*). J Phycol 18:483–488

Brown LM, Hellebust JA (1980) The contribution of organic solutes to osmotic balance in some green and eustigmatophyte algae. J Phycol 16:265–270

Busch KB, Fromm H (1999) Plant succinic semialdehyde dehydrogenase. Cloning, purification, pocalization in mitochondria, and regulation by adenine nucleotides. Plant Physiol 121:589–598

Chaturvedi V, Bartiss A, Wong B (1997) Expression of bacterial mtlD in *Saccharomyces cerevisiae* results in mannitol synthesis and protects a glycerol-defective mutant from high-salt and oxidative stress. J Bacteriol 179:157–162

Chen G-Q, Jiang Y, Chen F (2008) Salt-induced alterations in lipid composition of diatom *Nitzschia laevis* (*Bacillariophyceae*) under heterotrophic culture condition. J Phycol 44:1309–1314

Doyle JJ, Doyle JL (1987) A rapid DNA isolation procedure for small quantities of fresh leaf tissue. Phytochem Bull 19:11–15

Dittami SM, Gravot A, Goulitquer S, Rousvoal S, Peters AF, Bouchereau A, Boyen C, Tonon T (2012) Towards deciphering dynamic changes and evolutionary mechanisms involved in the adaptation to low salinities in *Ectocarpus* (brown algae). Plant J 71:366–377

Dörmann P, Benning C (2002) Galactolipids rule in seed plants. Trends Plant Sci 7:112–118

Fait A, Yellin A, Fromm H (2005) GABA shunt deficiencies and accumulation of reactive oxygen intermediates: insight from *Arabidopsis* mutants. FEBS Lett 579:415–420

Fait A, Fromm H, Walter D, Galili G, Fernie AR (2008) Highway or byway: the metabolic role of the GABA shunt in plants. Trends Plant Sci 13:14–19

Fawley KP, Fawley MW (2007) Observations on the diversity and ecology of freshwater *Nannochloropsis* (*Eustigmatophyceae*), with descriptions of new taxa. Protist 158:325–336

Fernandez O, Béthencourt L, Quero A, Sangwan RS, Clément C (2012) Trehalose and plant stress responses: friend or foe? Cell Mol Life Sci 69:3225–3243

Fietz S, Bleiß W, Hepperle D, Koppitz H, Krienitz L, Nicklisch A (2005) First record of *Nannochloropsis limnetica* (*Eustigmatophyceae*) in the autotrophic picoplankton from lake Baikal. J Phycol 41:780–790

Fisher T, Berner T, Iluz D, Dubinsky Z (1998) The kinetics of the photoacclimation response of *Nannochloropsis* sp. (*Eustigmatophyceae*): a study of changes in ultrastructure and PSU density. J Phycol 34:818–824

Garza–Sánchez F, Chapman DJ, Cooper JB (2009) *Nitzschia ovalis* (*Bacillariophyceae*) mono lake strain accumulates 1,4/2,5 cyclohexanetetrol in response to increased salinity. J Phycol 45:395–403

Ginzburg M, Ratcliffe R, Southon T (1988) Phosphorus metabolism and intracellular pH in the halotolerant alga *Dunaliella parva* studied by ^{31}P-NMR. Biochim Biophys Acta–Mol Cell Res 969:225–235

Guschina IA, Harwood JL (2009) Algal lipids and effect of the environment on their biochemistry. In: Kainz M, Brett M, Arts M (eds) Lipids in aquatic ecosystems. Springer, Dordrecht, pp 1–24

Gustavs L, Eggert A, Michalik D, Karsten U (2010) Physiological and biochemical responses of green microalgae from different habitats to osmotic and matric stress. Protoplasma 243:3–14

Harwood J (1998) Membrane lipids in algae. In: Siegenthaler P-A, Murata N (eds) Lipids in photosynthesis: structure, function and genetics. Kluwer, Netherlands, pp. 53–64.

Henley WJ, Major KM, Hironaka JL (2002) Response to salinity and heat stress in two halotolerant chlorophyte algae. J Phycol 38:757–766

Hibberd D (1981) Notes on the taxonomy and nomenclature of the algal classes *Eustigmatophyceae* and *Tribophyceae* (synonym *Xanthophyceae*). Bot J Linn Soc 82:93–119

Huflejt ME, Tremolieres A, Pineau B, Lang JK, Hatheway J, Packer L (1990) Changes in membrane lipid composition during saline growth of the fresh water cyanobacterium *Synechococcus* 6311. Plant Physiol 94:1512–1521

Ishitani M, Majumder AL, Bornhouser A, Michalowski CB, Jensen RG, Bohnert HJ (2002) Coordinate transcriptional induction of myo-inositol metabolism during environmental stress. Plant J 9:537–548

Jarvis P, Dörmann P, Peto CA, Lutes J, Benning C, Chory J (2000) Galactolipid deficiency and abnormal chloroplast development in the *Arabidopsis* MGD synthase 1 mutant. Proc Natl Acad Sci USA 97:8175–8179

Jinkerson R, Radakovits R, Posewitz MC (2013) Genomic insights from the oleaginous model alga *Nannochloropsis gaditana*. Bioengineered 4:37–43. doi:10.4161/bioe.21880

Kasukabe Y, He L, Nada K, Misawa S, Ihara I, Tachibana S (2004) Overexpression of spermidine synthase enhances tolerance to multiple environmental stresses and up-regulates the expression of various stress-regulated genes in transgenic *Arabidopsis thaliana*. Plant Cell Physiol 45:712–722

Khozin-Goldberg I, Didi-Cohen S, Shayakhmetova I, Cohen Z (2002) Biosynthesis of eicosapentaenoic acid (EPA) in the freshwater eustigmatophyte *Monodus subterraneus* (*Eustigmatophyceae*). J Phycol 38:745–756

Kirst G (1989) Salinity tolerance of eukaryotic marine algae. Annu Rev Plant Physiol Plant Mol Biol 41:21–53. doi:10.1146/annurev.pp.41.060190.000321

Krienitz L, Hepperle D, Stich HB, Weiler W (2000) *Nannochloropsis limnetica* (*Eustigmatophyceae*), a new species of picoplankton from freshwater. Phycologia 39:219–227

Lisec J, Schauer N, Kopka J, Willmitzer L, Fernie AR (2006) Gas chromatography mass spectrometry-based metabolite profiling in plants. Nat Protoc 1:387–396

Liu CH, Shih MC, Lee TM (2000) Free proline levels in *Ulva* (*Chlorophyta*) in response to hypersalinity: elevated NaCl in seawater versus concentrated seawater. J Phycol 36:118–119

Lu N, Wei D, Chen F, Yang ST (2012) Lipidomic profiling and discovery of lipid biomarkers in snow alga *Chlamydomonas nivalis* under salt stress. Eur J Lipid Sci Technol 114:253–265

Luedemann A, Strassburg K, Erban A, Kopka J (2008) TagFinder for the quantitative analysis of gas chromatography–mass spectrometry (GC–MS)-based metabolite profiling experiments. Bioinformatics 24:732–737

Lunn JE, Feil R, Hendriks JH, Gibon Y, Morcuende R, Osuna D, Scheible W-R, Carillo P, Hajirezaei M-R, Stitt M (2006) Sugar-induced increases in trehalose 6-phosphate are correlated with redox activation of ADPglucose pyrophosphorylase and higher rates of starch synthesis in *Arabidopsis thaliana*. Biochem J 397:139–148

Miller G, Honig A, Stein H, Suzuki N, Mittler R, Zilberstein A (2009) Unraveling Δ1-pyrroline-5-carboxylate-proline cycle in plants by uncoupled expression of proline oxidation enzymes. J Biol Chem 284:26482–26492

Obata T, Fernie AR (2012) The use of metabolomics to dissect plant responses to abiotic stresses. Cell Mol Life Sci 69:3225–3243

Pal D, Khozin-Goldberg I, Cohen Z, Boussiba S (2011) The effect of light, salinity, and nitrogen availability on lipid production by *Nannochloropsis* sp. Appl Microbiol Biotechnol 90:1429–1441

Recht L, Zarka A, Boussiba S (2012) Patterns of carbohydrate and fatty acid changes under nitrogen starvation in the microalgae *Haematococcus pluvialis* and *Nannochloropsis* sp. Appl Microbiol Biotechnol 94:1495–1503

Renaud S, Parry D (1994) Microalgae for use in tropical aquaculture. II: Effect of salinity on growth, gross chemical composition and fatty acid composition of three species of marine microalgae. J Appl Phycol 6:347–356

Renaud S, Parry D, Thinh L, Kuo C, Padovan A, Sammy N (1991) Effect of light intensity on the proximate biochemical and fatty acid composition of *Isochrysis* sp. and *Nannochloropsis oculata* for use in tropical aquaculture. J Appl Phycol 3:43–53

Rodolfi L, Zittelli GC, Bassi N, Padovani G, Biondi N, Bonini G, Tredici MR (2009) Microalgae for oil: strain selection, induction of lipid synthesis and outdoor mass cultivation in a low-cost photobioreactor. Biotechnol Bioeng 102:100–112

Roessner U, Willmitzer L, Fernie AR (2001) High-resolution metabolic phenotyping of genetically and environmentally diverse potato tuber systems. Identification of phenocopies. Plant Physiol 127:749–764

Schneider JC, Roessler P (1994) Radiolabeling studies of lipids and fatty acids in *Nannochloropsis* (*Eustigmatophyceae*), an oleaginous marine alga. J Phycol 30:594–598

Simionato D, Sforza E, Carpinelli EC, Bertucco A, Giacometti GM, Morosinotto T (2011) Acclimation of *Nannochloropsis gaditana* to different illumination regimes: effects on lipids accumulation. Bioresour Technol 102:6026–6032

Solovchenko A, Khozin-Goldberg I, Recht L, Boussiba S (2011) Stress-induced changes in optical properties, pigment and fatty acid content of *Nannochloropsis* sp.: implications for non-destructive assay of total fatty acids. Mar Biotechnol 13:527–535

Stefanov K, Seizova K, Elenkov I, Kuleva L, Popov S, Dimitrova-Konaklieva S (1994) Lipid composition of the red *alga Chondria tenuissima* (Good et Wood.) Ag., inhabiting waters with different salinities. Bot Mar 37:445–448

Suda S, Atsumi M, Miyashita H (2002) Taxonomic characterization of a marine *Nannochloropsis* species, *N. oceanica* sp. nov. (*Eustigmatophyceae*). Phycologia 41:273–279

Sukenik A (1999) Production of EPA by *Nannochloropsis*. In: Cohen Z (ed) Chemicals from microalgae. Taylor and Francis, London, pp 41–56

Sukenik A, Beardall J, Kromkamp JC, Kopeck J, Masojídek J, van Bergeijk S, Gabai S, Shaham E, Yamshon A (2009) Photosynthetic performance of outdoor *Nannochloropsis* mass cultures under a wide range of environmental conditions. Aquat Microb Ecol 56:297–308

Sukenik A, Yamaguchi Y, Livne A (1993a) Alterations in lipid molecular species of the marine eustigmatophyte *Nannochlorosis* sp. J Phycol 29:620–626

Sukenik A, Zamora O, Carmeli Y (1993b) Biochemical quality of marine unicellular algae with emphasis on lipid composition. II. *Nannochlorosis* sp. Aquaculture 117:313–326

Vieler A, Wu G, Tsai CH, Bullard B, Cornish AJ, Harvey C, Reca IB, Thornburg C, Achawanantakun R, Buehl CJ, Campbell MS, Cavalier D, Childs KL, Clark TJ, Deshpande R, Erickson E, Armenia

Ferguson A, Handee W, Kong Q, Li X, Liu B, Lundback S, Peng C, Roston RL, Sanjaya, Simpson JP, Terbush A, Warakanont J, Zäuner S, Farre EM, Hegg EL, Jiang N, Kuo MH, Lu Y, Niyogi KK, Ohlrogge J, Osteryoung KW, Shachar-Hill Y, Sears BB, Sun Y, Takahashi H, Yandell M, Shiu SH, Benning C (2012) Genome, functional gene annotation, and nuclear transformation of the heterokont oleaginous alga *Nannochloropsis* sp.CCMP1779. PLoS Genet 8:e1003064. doi: 10.1371/journal.pgen.1003064

Zhifang G, Loescher W (2003) Expression of a celery mannose 6–phosphate reductase in *Arabidopsis thaliana* enhances salt tolerance and induces biosynthesis of both mannitol and a glucosyl–mannitol dimer. Plant Cell Environ 26:275–283

Zou N, Zhang C, Cohen Z, Richmond A (2000) Production of cell mass and eicosapentaenoic acid (EPA) in ultrahigh cell density cultures of *Nannochloropsis* sp. (*Eustigmatophyceae*). Eur J Phycol 35:127–133